Design, Simulation and Fabrication of Silicon Microneedles for Bio-Medical Applications

Muhammad Waseem Ashraf [1], **Shahzadi Tayyaba**[2], **Nitin Afzulpurkar**[3], **Asim Nisar**[4], **Erik Lucas Julien Bohez**[5], **Tanom Lomas**[6], and **Adisorn Tuantranont**[7], Non-members

ABSTRACT

In this paper, design, analysis and fabrication of hollow out-of-plane silicon microneedles for transdermal drug delivery (TDD) have been presented. Combination of isotropic and anisotropic etching process has been used to facilitate the fabrication of microneedles in inductively coupled plasma (ICP) etcher. Using ANSYS, structural and microfluidic analysis has been performed before the fabrication to insure the microneedle design suitability for TDD. In finite element analysis (FEM), the effect of axial and transverse load on single microneedle has been investigated to envisage the mechanical properties of microneedle. The analysis predicts that the resultant stresses due to applied bending and axial loads are in the safe range. In computational fluid dynamic (CFD) static analysis, the fluid flow rate through 5×5 microneedle array has been investigated by applying the pressure 10 kPa to 130 kPa at the inlet to insure that the microneedles are capable for flow of drug up to the desired range for TDD.

Keywords: Silicon Microneedles, Transdermal Drug Delivery, Structural Analysis, Computational Fluid Dynamic Analysis, Inductively Coupled Plasma Etching

1. INTRODUCTION

Transdermal drug delivery (TDD) has been considered as a patient-friendly method in delivery of pharmaceutical compounds by eradicating pain, gastrointestinal absorption, liver metabolism and degradation that are associated with conventional drug delivery approaches such as hypodermic injections and oral administration of drugs. Drug delivery devices using Micro and Nano electromechanical systems (MEMS and NEMS) technology are progressively being developed for biomedical applications. The main advantage of the MEMS based drug delivery system is the ease of mass fabrication of small feature sizes at low cost and making such systems desirable for commercial applications.

TDD devices can be divided into active and passive devices based on the technologies used for skin permeation. In passive devices, the methods used for skin permeation are chemical enhancers, emulsions, and lipid assemblies as well as biological methods such as peptides [1, 2, 3]. The most common active methods of skin permeation are iontophoresis, ultrasound, jet injectors, electroporation, microneedles, powder injection, ablation, and tape stripping [4]. One of the major drawbacks of TDD systems has been their inability to deliver the drugs through the skin within the desired therapeutic range. To overcome this limitation, many studies have been conducted on new drug delivery methods using emerging micro and nanotechnologies. The major focus of MEMS for drug delivery has been towards the development of microneedles for minimally invasive TDD applications. Many developments in the use of micron size needles have been reported recently to dramatically increase transdermal delivery. A microneedle array is one of the most recent methods for drug delivery. It combines the concepts of drug delivery across the skin using patches and hypodermic injections [5].

A MEMS based microneedle is a needle with diameter and length in micrometers. A microneedle is different from standard hypodermic needles used in medical applications as generally the length of the MEMS based microneedles is less than 1 mm [6]. Thus microneedles are significantly smaller in length than ordinary needles. Microneedle arrays based devices currently find their way into many applications in biomedical. The microneedles are used to penetrate the outer layer of skin and generate pathways for drug into the epidermis layer. It causes no pain induction as the needles have a short length and they do not arrive at nerves in deeper dermis layer [7]. Microneedles have been fabricated for various purposes. Microneedles with lumen and reservoir were developed for local delivery with precise dose and controlled release [8]. The idea of using microneedles for

Manuscript received on July 27, 2010 ; revised on October 19, 2010.

This paper is extended from the paper presented in ECTICON 2010.

[1,2,3,4,5] The authors are with School of Engineering and Technology, Asian Institute of Technology (AIT), Bangkok, Thailand, E-mail: Muhammd.Waseem.Ashraf@ait.ac.th, shahzadi_tayyaba@ait.ac.th, Nitin@ait.ac.th, Asim.Nisar@ait.ac.th and bohez@ait.ac.th

[6,7] The authors are with 2Nanoelectronics and MEMS Lab, National Electronics and Computer Technology Center (NECTEC), Thailand, E-mail: Tnom.Lomas@nectec.org.th and Adisorn.Tuantranont@nectec.org.th

drug delivery on skin was presented in 1976 by Alza Corporation [9], but it was not displayed experimentally until 1990s. The microneedles are classified as in-plane and out-of-plane microneedles based on the fabrication process. A schematic illustration of in-plane and out-of-plane microneedles is shown in Fig. 1. In in-plane microneedles, the microneedle shaft is parallel to the substrate surface. In out-of-plane microneedles, the length of the microneedles protrudes out of the substrate surface.

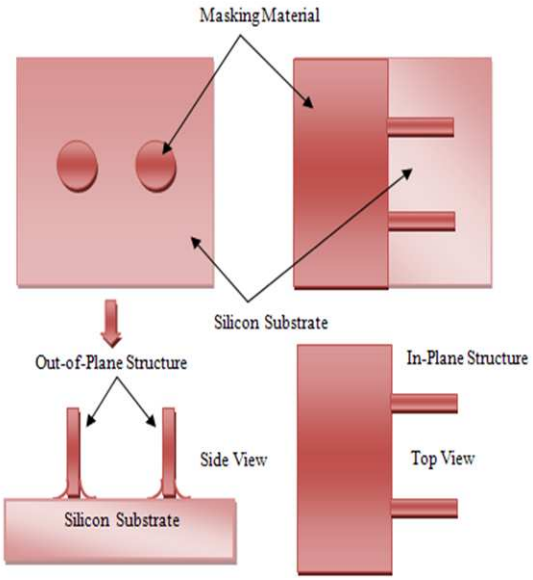

Fig.1: *In-plane and Out-of-plane Microneedles Structure*

According to the geometry, the microneedles can be solid or hollow. In hollow microneedles, an internal lumen is present which allows fluid flow through the microneedles. Microneedles have also been made by metal, polymer, etc. Each material has its own advantages and limitations. Microneedles also vary according to structure, tip shape and over all shape. The detail of microneedles categories is shown in Table1.

Table 1: *Performance comparisons in term of peak and average values*

Material	Overall Shape	Tip shape	Structure
Silicon	Cylindrical	Volcano	Solid
Silicon dioxide	Pyramid	Snake fang	Hollow
Silicon Nitride	Candle	Micro-hypodemis	In-plane
Glass	Spike		Out-of-plane
Semiconductor	Spear		
Metal	Square		
Alloys			
Polymers			

The earliest out-of-plane microneedle array consisted of 100 microneedles with a length of 1.5 mm was reported in 1991 [10]. Design and development of MEMS based microneedles are strongly dependent on the fabrication process. A wide variety of fabrication technologies have been existed today and majority of these technologies have been derived from processes developed to fabricate integrated circuits. Few of them have been reported in literature to fabricate microneedles like photolithography [11], deep x-ray lithography [12], deep reactive ion etching (DRIE) [13], micro-molding [14], bi-mask technique [15], surface micromachining [16], LIGA [17], hot embossing [18], UV excimer laser [19], laser micromachining [20], coherent porous silicon etching (CPS) [21], injection molding [22], and micropipette pulling technique [23]. In these processes, silicon and polymer can be used as substrate materials for microneedles fabrication. Following researchers have used silicon as substrate material to fabricate the microneedles [24-30]. The application of silicon as the substrate material is still dominant because of some excellent mechanical properties, electrical properties and possibility to directly integrate circuit on the transducer's substrate.

With the help of anisotropic etching process, deep holes or free standing structures can be fabricated in silicon. These high aspect ratio structures are of considerable interest in developing micro size devices for various applications. This process of fabrication is generally referred to as deep reactive ion etching (DRIE) process. Silicon is anisotropically etched by DRIE process in a commercially available etching machine called inductively coupled plasma (ICP) etcher. ICP etcher fabrication process involves a plasma source and a combination of sequential etching and polymer deposition. With the help of ICP etching, high aspect ratio structures up 30:1 can be achieved. ICP etcher uses SF6 gas for etching cycle and C4F8 gas for passivation cycle. DRIE using ICP etcher is commonly called the BOSCH process. In ICP etching process, plasma and gas pressure/flow parameters need to be controlled to achieve desired etch characteristics and profile.

The most significant work on microneedles for transdermal drug delivery applications began in 1998 when fabrication of 150 ?m long solid silicon microneedles was reported using DRIE process [31]. Biodegradable polymer microneedles were fabricated by vacuum casting of polyglycolic acid in a silicon mold [32]. Hollow microneedles with reservoirs have been developed for transdermal drug delivery to eliminate problem of fluctuation in daily dosage to reduce side effects [33]. Out-of-plane hollow metallic microneedles were fabricated with SU-8 mold and backside exposure by metal deposition technology [34]. Inclined LIGA process was developed to fabricate microneedle array using polymethyl methacrylate (PMMA) [35]. Micromachining methods in metal and polymer have their own limitations. Therefore, the above mentioned methods are complicated to fabricate microneedles. Silicon as substrate has been widely used to fabricate the out-of-plane microneee-

dles for drug delivery applications.

In this work authors present the design, structural analysis, microfluidic analysis and fabrication of cylindrical silicon hollow out-of-plane microneedle array for drug delivery applications. Using ANSYS, structural and computational fluid dynamic (CFD) static analysis have been conducted before the fabrication to envisage the suitability of microneedles design for drug delivery. Mechanical strength of microneedles and fluid flow rate through the microneedles have been investigated in the structural and microfluidic analysis. The present study provides useful predicted data to fabricate suitable drug delivery device.

2. FABRICATION PROCESS

The proposed fabrication process of microneedles and reservoir involves isotropic and anisotropic etching processes using standard silicon wafers. The desired shape of microneedle structures is achieved by controlling the etch times at various processing steps. Three set of chrome masks have been fabricated. Microneedle Mask MN1 has been used to fabricate microneedle outside shape. Microneedle mask MN2 has been used to fabricate inner hole called lumen while the third microneedle Mask MN3 has been used for backside reservoir etching. The fabrication process involves many steps. The stepwise fabrication process of microneedles is shown in Fig. 2. The first step involves wafer cleaning of single sided polished 6" Si wafer with Piranha solution and de-ionized (DI) water (Figure 2 a). The silicon wafer is then blown dry with air gun. The second step is to cap photoresist mask (Fig. 2 b). This step involves various sub steps such as spin coating photoresist AZ4620 3000 rpm, soft bake (120-180 sec 110 °C, expose wafer, develop in developer solution AZ 400K and hard bake. Then isotropic silicon dry etching of silicon wafer with ICP etch tool is done using SF_6/O_2 gases for outside shape of microneedle tips in standard photolithography process (Etch depth = 15 μm) (Fig. 2 c). Then photoresist is stripped off and wafer is cleaned. The next step is to thermally grow silicon oxide layer on both sides of the wafer in oxidation furnace by wet oxidation at 1000 °C.

Then each side of wafer is protected by capping with another wafer for mask oxide etching and then photoresist is striped off. To perform first ICP etching, the photoresist is first coated with 5 μm thickness. The etching depth for first ICP etch is 150 μm (Fig. 2 d). This is followed by second ICP etch up to 200 μm. Then wafer is caped with another mask (Fig. 2 e) and third ICP etching is done to make the reservoir on the backside of the wafer (Fig. 2 f). The final steps involve release, oxide etch and dicing. The fabricated microneedles are shown in results and discussion section of the paper.

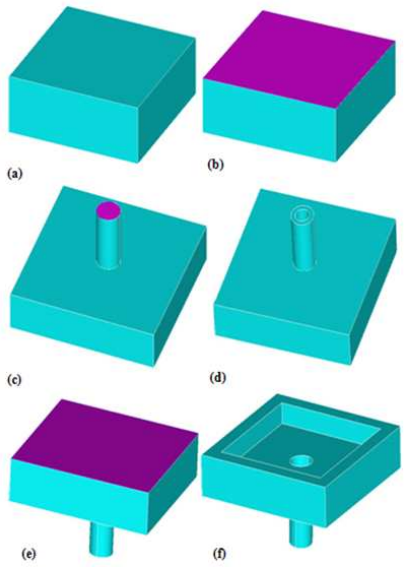

Fig.2: *Fabrication Process of Hollow Silicon Out-of-plane Microneedles*

3. THEORETICAL ANALYSIS

3.1 Mechanical Design of Microneedle

The microneedle design is cylindrical. L presents the length of microneedle that is limited up to 200 μm. The internal diameter (Di) of microneedle is 60 μm and outer diameter (Do) of microneedle is 150 μm. Pi and Po represent the inlet and outlet pressures. Q presents the flow rate. The centre-to-centre distance of the microneedle in array is 1000 ?m. The fluid reservoir is designed on the backside of the microneedle. A schematic illustration of the design of single microneedle is shown in Fig. 3.

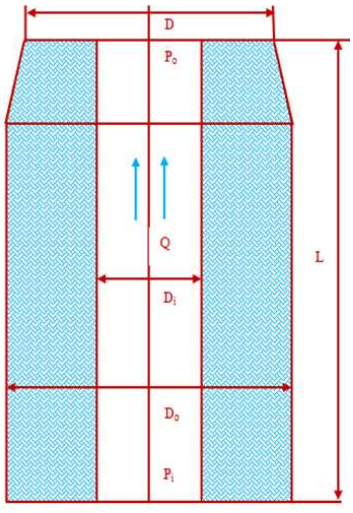

Fig.3: *Design Specification of Single Silicon Microneedle*

3.2 Microneedle Mechanics

The microneedles experience resistive forces by skin when inserted into skin. Therefore, in order to penetrate the microneedle into the skin, the applied axial force on microneedle should be greater than the skin resistive forces. An axial force acts on the microneedle tip during insertion. This axial force is compressive and causes buckling of the microneedle. Failure of microneedle is possible during skin insertion due to bending or buckling. The axial force can be reduced by decreasing the tip area of the microneedle. As buckling is directly related with compressive force, which acts during insertion, sharp microneedle tip reduces buckling. Hence insertion of microneedle into the skin becomes easy. The bending may also occur due to uneven surface of skin or human error. Hence, the design of microneedle is important for proper delivery without any failure. The axial force (compressive force) which the microneedle can withstand without breaking is given by (1).

$$F_{compressive} = \sigma_y A \tag{1}$$

Where, σ_y is yield strength, and A is cross sectional area of the microneedle tip which is very small.

The cross sectional area of hollow cylindrical section is $A = \frac{\pi}{8}(D_0^4 - D_i^4)$. Where, D_o is the outer diameter and D_i is the inner diameter of the hollow cylindrical section of microneedles. The yield strength of silicon is 7 GPa.

$$F_{Buckling} = \frac{\pi^2 EI}{L^2} \tag{2}$$

Where, E is young's modulus, I is moment of inertia, and L is length of the microneedle. Moment of inertia for the hollow cylindrical section is $I = \frac{\pi}{64}(D_o^4 + D_i^4)$.

Needle always penetrate into the skin with particular angle. There is a risk involve in microneedles fracture during skin puncturing. The bending force at which the microneedle can withstand without breaking is given by (3).

$$F_{Bending} = \frac{\sigma_y I}{cL} \tag{3}$$

Where, $c = \frac{D}{2}$ is the distance from vertical axis to the outer edge of the section.

3.3 Microfluidic Analysis

The design of microneedle is cylindrical, so Poiseulle's law is considered to measure the fluid flow through microneedle array during microfluidic analysis and given as:

$$Q' = \frac{\pi D_i^4 V P}{64 \mu L} \tag{4}$$

Where, Q' is the flow rate, D_i is the inner diameter of microneedle and ? is the viscosity.

Modified Bernoulli equation is considered to model the geometry of microneedles. The pressure loss is calculated by considering the friction losses and given by [38]:

$$\frac{P_1}{pg} + \frac{V_1}{2g} + Z_1 = \frac{P_2}{pg} + \frac{V_2}{2g} + Z_2 + \frac{fl}{d} + \frac{V^2}{2g} + \sum \frac{KV^2}{2g} \tag{5}$$

Where, P_1 is inlet pressure, P_2 is outlet pressure, V_1 is inlet velocity, V_2 is outlet velocity and f is friction factor.Since the cylindrical section is symmetrical about a vertical axis, the outlet pressure, velocity and the distances (Z1 and Z2) remain the same. The friction factor for laminar flow is given as $f = \frac{64}{Re}$[38].

4. NUMERICAL SIMULATION

Using ANSYS, two different types of simulations have been conducted before the fabrication of microneedles to envisage the suitability of microneedles design for drug delivery. Single microneedle was modelled in structural analysis to investigate the mechanical properties of microneedle. In microfluidic analysis the fluid flow rate was investigated through 5?5 microneedle array. Finite element method (FEM) has been used in these analyses.

4.1 Structure Analysis

FEM was used to perform the structural analysis of the microneedle. During skin insertion, microneedle experiences various forces such as axial force, bending force, shear force etc. Single out-of-plane microneedle was modelled with fixed base and free tip end for the bending and axial stress analysis. The structural model was built by using element SOLID 95, which is mostly used to model silicon material. Linear isotropic material properties of silicon were used for FEM analysis. The Young modulus of 169 GPa and Poisson ratio of 0.22 were considered for structure analysis. The fracture strength of silicon is 7 GPa that has been considered during structural analysis of microneedles [38]. In the simulation study, bending and axial stress analyses were performed by applying transverse and axial loads respectively. The range of transverse load is assumed according to the fracture strength of the material and can be calculated from equation 3. For the microneedle failure analysis, stress at the fixed end (bottom) of the microneedle was taken into consideration. Fig. 4 shows the simulation result at the bottom of the microneedle for the applied bending force of 8.2 N at the tip.

It was found in the numerical solution that the maximum stress of 5.05 GPa occurs at the bottom of the microneedle for the applied bending force, which is below the yield stress of the material. The skin offers resistive forces during skin puncturing. The value of that resistive force is 3.18 MPa [39]. Hence, to overcome this skin resistance, the microneedle must

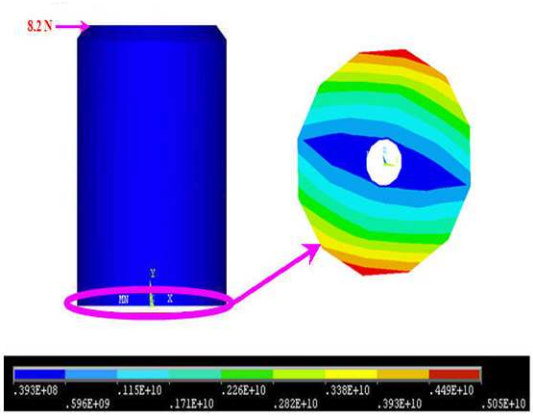

Fig.4: *Bending Stress Analysis*

withstand the load more than 3.18 MPa. To show the effect of this resistive forces on the structure of the microneedle, FEM analysis was performed. The effect of applied axial load on the free end of the microneedle is shown in Fig. 5. The maximum stress occurs inside the lumen section of the microneedle, which is well below the yield stress limit with negligible deflection. The result shows that the microneedle design is strong enough to penetrate into the human skin without failure.

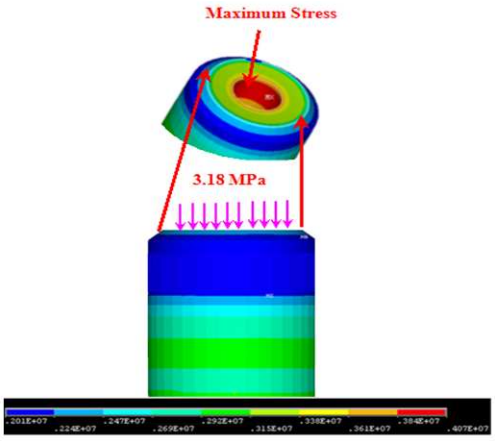

Fig.5: *Axial Stress Analysis*

4.2 Microfluidic CFD Static Analysis

In this simulation, CFD static analysis has been performed to predict the fluid flow rate through the microneedle array. The pressures of 10 kPa to 130 kPa were applied on the inlet of microneedles. Acetone was considered as working fluid in fluid domain. The outlet pressure was assumed to be zero. The friction factor 0.05 has been considered during fluidic analysis. The pressure distribution through 5×5 microneedle array at applied pressure of 130 kPa is shown in Fig.6.

The maximum fluid pressure of $1.036e^5$ has been

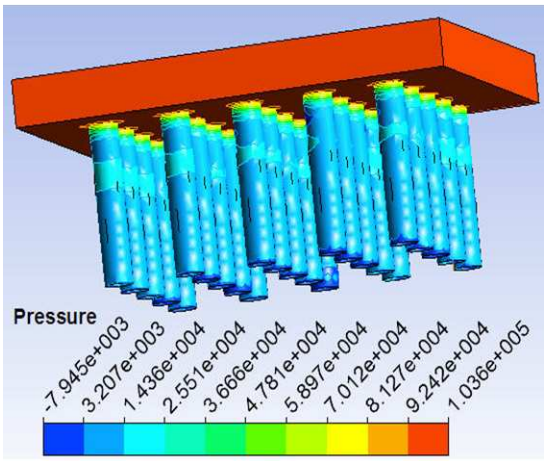

Fig.6: *Pressure Distribution for* 5×5 *Microneedles Array*

observed through each microneedle. Simulation results shows that the fluid flow is uniform through each microneedle. Fig. 7 shows 3D view of fluid flow through the microneedles during CFD static analysis. The velocity profile in CFD static analysis at the applied pressure of 130 kPa is shown in Fig. 8.

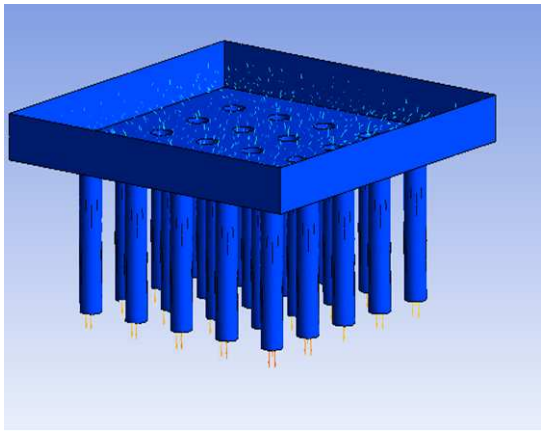

Fig.7: *3D View of Fluid Flow through Microneedle*

The maximum fluid velocity of $1.458e^1$ was observed through each microneedle in CFD static analysis. The velocity of fluid increases in the microneedle lumen section due to small area and zero pressure at the outlet. Due to frictional losses between fluid and wall, the velocity of the fluid is less at the wall area of the lumen as compared to the central region of the lumen section.

5. RESULTS AND DISCUSSIONS

In this work the simulation and fabrication of microneedles have been presented. The simulation has been conducted using finite element software ANSYS. Microfluidic and structural analysis have been performed in simulation. Various forces have been in-

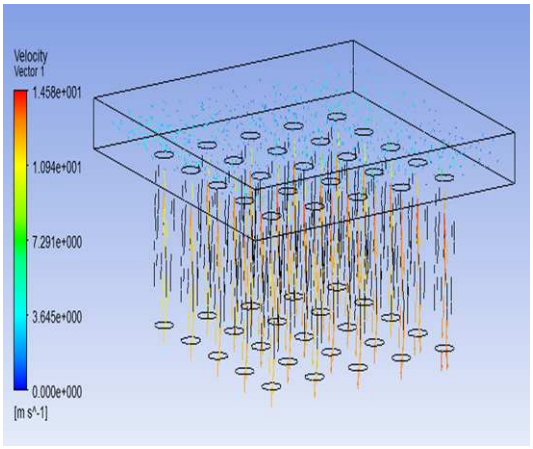

Fig.8: *Velocity Profile in CFD Static Analysis*

fluenced by microneedles during skin penetration like bending, resistive, buckling, lateral and compressive forces. The structural analysis has been performed in ANSYS to predict the effect of these forces for the proposed design. In structural analysis, the deflection along the length of microneedle at applied force 8.2 N is shown by Fig. 9.

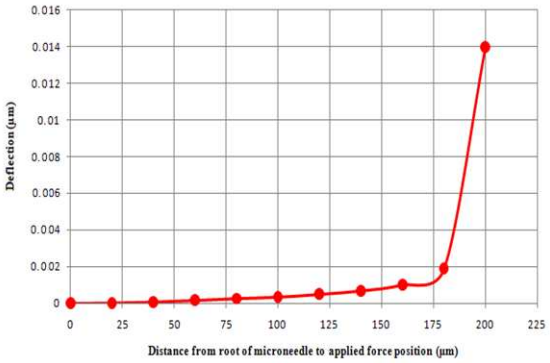

Fig.9: *Deflection along the Length of Microneedle*

Microfluidic analysis has been conducted to investigate the fluid flow through the lumen section of microneedles using ANSYS. The pressure drop in the lumen section can also be calculated by using equation 5. In microfluidic analysis friction factor was considered 0.05. In static CFD analysis, the relationship between pressure and velocity of fluid is shown in Fig. 10.

In CFD static analysis, the variation in the fluid velocity along the length of microneedle is shown in Fig. 11.

The variation in the fluid pressure along the length of microneedle is shown in Fig. 12.

Hollow out-of-plane silicon microneedle array has been fabricated successfully using a series of combined isotropic and anisotropic etching processes in ICP etching machine. Wet etching was used for front and back side mask oxide etching. The microneedle

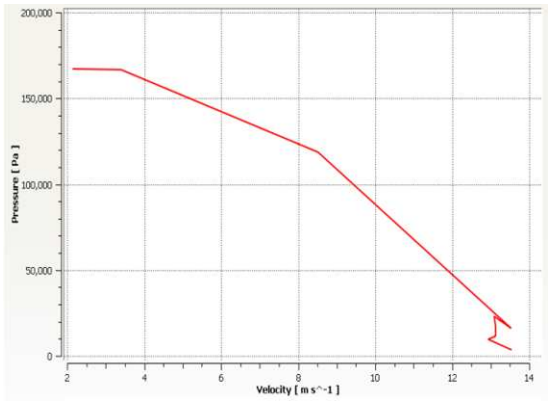

Fig.10: *Pressure Vs Velocity in Static Analysis*

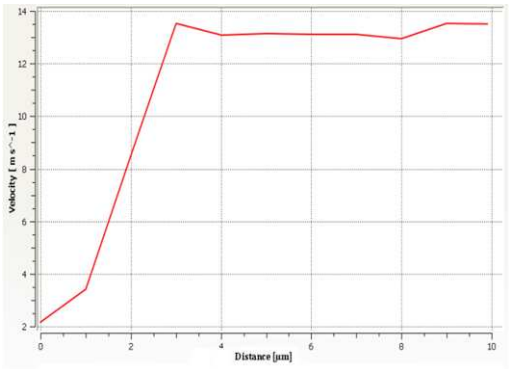

Fig.11: *Velocity Variations in CFD Static Analysis*

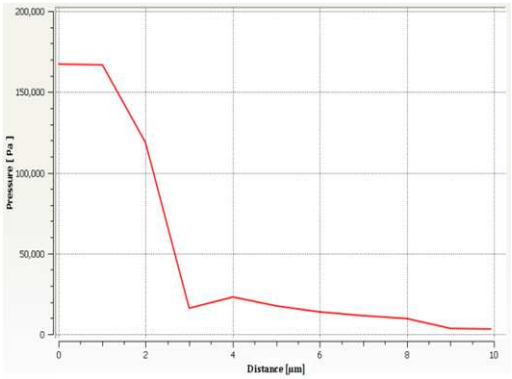

Fig.12: *Pressure Variations in CFD Static Analysis*

tip was fabricated by isotropic etching using SF_6/O_2 gases in ICP etcher. The BOSCH process was used for outer vertical shape, lumen and backside etching. The scanning electron microscope (SEM) image of the fabricated microneedle array is shown in Fig. 13.

Different researchers have been involved in testing of microneedles on chicken skin [40], mouse skin [41] and human skin [42]. In this work the successful fabrication of hollow out-of-plane silicon microneedles has been done. The simulation results show that the design of fabricated microneedles is suitable for biomedical applications. The testing of fabricated mi-

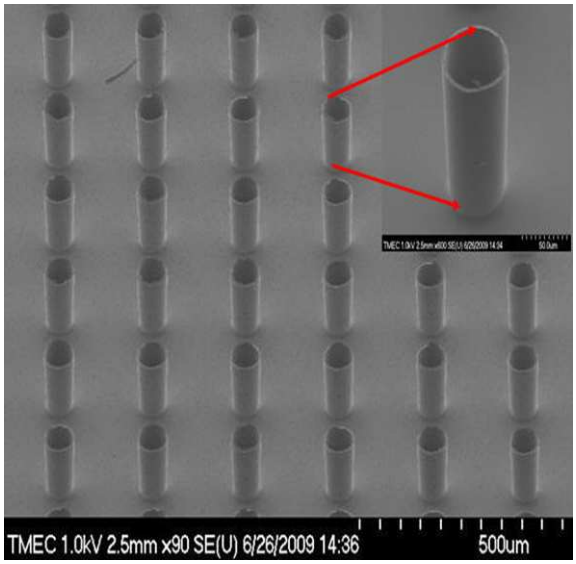

Fig.13: *SEM Image of Silicon Microneedle Array*

croneedles will be performed and presented in future work.

6. CONCLUSION

This paper presents the simulation and fabrication of high aspect ratio hollow out-of-plane silicon microneedle array for transdermal drug delivery and other biomedical applications. The fabrication process of hollow silicon microneedles involves combination of isotropic and anisotropic etching process using ICP etching technology. The structural analysis of silicon microneedles using ANSYS has been performed to predict the stress distribution. Simulation results show that the maximum stress of 5.05 GPa occurs at the bottom of the microneedle for the applied bending force of 8.2 N, which is below the yield stress of the material. The CFD static analysis has been conducted to predict the fluid flow rate through the 5×5 microneedle array. The presented research work provides useful information and predicted data to fabricate optimized designs of hollow out-of-plane silicon microneedle array for biomedical applications.

7. ACKNOWLEDGEMENT

The authors would like to thank and acknowledge K. Saejok, C. Hruanun, Atthi N. Somwamg, and J. Supadech at Thai Microelectronics Center (TMEC), Thailand for providing DRIE facility and process for microneedle fabrication. The first author Mr. Muhammad Waseem Ashraf is also thankful to Higher Education Commission (HEC) Pakistan for providing fund for PhD at Asian Institute of Technology (AIT), Bangkok, Thailand.

References

[1] M. R. Prausnitz, "Microneedles for transdermal drug delivery," *Adv Drug Deliv Rev.* Vol. 56, pp. 581-587, 2004.

[2] YB Scuetz, A. Naik, RH. Guy, and YN Kalia, "Emerging strategies for the transdermal delivery of peptide and protein drugs," *Expert Opin. Drug Deliv.* Vol. 2, pp. 533-548, 2005.

[3] P. Karande, A. Jain, and S. Mitragotri, "Discovery of transdermal penetration enhancers by high- throughput screening," *Nat. Biotechnol.* Vol. 22, pp. 192-197, 2004.

[4] A. Arora, MR. Prausnitzc, and S. Mitragotri, "Micro-scale devices for transdermal drug delivery," *Int. J. Pharm.* Vol. 364. pp. 227-236, 2008.

[5] B. A. Qallaf and D. B. Das, "Optimization of square microneedle arrays for increasing drug permeability in skin," *Chemical Engieering Sci* Vol. 63, pp 2523-2535, 2008.

[6] D. W. Bodhale, A. Nisar, N. Afzulpurkar, "Structural and microfluidic analysis of hollow side-open polymeric microneedles for transdermal drug delivery applications," *Microfluid Nanofluid*, Vol. 8, pp. 373-392, 2010.

[7] B. Chen. J. Wei, F. E. H. Tay, W, Y. T. Wong, and C. Iliescu, "Silicon microneedle array with biodegradable tips for transdemal drug delivery," *Microsyst Techno 14*, pp. 1015-1019, 2008.

[8] J. Ji, F. Tay, and J. Miao, "Microfabricated Hollow Microneedle Array Using ICP Etcher," *Journal of Physics, Confirence series 34*, pp. 1132-136, 2006.

[9] M.S. Gerstel, and V.A. Place, "Drug Delivery Device," US 3 964 482 patent, 1976.

[10] P. K. Campbell, K. E. Jones, R. J. Huber, K. W. Horch and R. A. Normann, "A silicon-based three-dimensional neural interface: manufacturing processes for an intracortical electrode array," *IEEE Trans Biomed Eng 38(8)*, 1991, pp.758-768.

[11] T. Shibata, A. Nakanishi, T. Sakai, N. Kato, T. Kawashima, T. Mineta, and E. Makino, "Fabrication and mechanical characterization of microneedle array for for cell surgery," In: *Actuators and Microsystems Conference*, pp 719-722.

[12] S. Khumpuang1, M. Horade, K. Fujioka, and S. Sugiyama, "Geometrical Strengthening and tip-sharping of a microneedle array fabricated by X-ray lithography," *Microsist Technol.* Vol. 13, pp. 209-214.

[13] L. M. Yu, F. E. H. Tay, D. G. Guo, L. Xu, K. L. Yap, "A microfabricated electrode with hollow microneedles for ECG measurements," *Sens Actuator A 151*, pp. 17-22, 2009.

[14] JW. Lee, JH. Park, MR. Prausnitz, "Dissolving microneedles for transdermal drug delivery," *Biomaterials.* Vol. 29, pp. 2113-2124, 2009.

[15] P. Zhang , C. Dalton, and G. A. Jullien, "De-

sign and fabrication of MEMS-based microneedles arrays for medical applications," *Microsyst Technol 15*, pp. 1073-1082, 2009.

[16] Z. Ding, F. J. Verbaan, M. Bivas-Benita, L. Bungener, A. Huckriede, D. J. van den Berg, G. Kersten, J. A. Bouwstra, "Microneedles arrays for the transcutaneous immunization of diphtheria and influenza in BALB/c mice," *J Control Release*. Vol. 136, pp. 71-78, 2009.

[17] S. P. Davis, W. Martanto, M. G. Allen, and M. R. Prausnitz, "Hollow metal microneedles for insulin delivery to diabetic rats," *IEEE Trans Biomed Eng 52(5)*, pp. 909-915.

[18] J. Oh , H. Park, K. Doa, M. Han, D. Hyun, C. Kim, C. Kim, S. S. Lee, S. Hwang, S. Shin, C. Cho, "Influence of the delivery systems using a microneedle array on the permeation of a hydrophilic molecule, calcein," *Eur. J. Pharm. Biopharm*. Vol. 69, pp. 1040-1045, 2009.

[19] M. W. Ashraf, S. Tayyaba, N. Afzulpurkar, "MEMS based Polymeric Drug Delivery System," CASE 2010, 6th IEEE Conference on Automation Science and Engineering, August 21-24, 2010, Toronto, Canada.

[20] R. Bhandari, S. Negi, L. Rieth, R. A. Norman, and F. Solzbacher, "A Novel Mask-Less Method of Fabricating High Aspect Ratio Microneedles for Blood Sampling," In: *IEEE, 2008 Electronic Components and Technology Conference*. 1306-1309.

[21] S. Rajaraman, and H. T. Henderson, "A unique fabrication approach for microneedles using coherent porous silicon technology," *Sens. Actuator B 105*, pp. 443-448.

[22] F. Sammoura, J. Kang, Y. Heo, T. Jung and L. Lin, "Polymeric microneedle fabrication using a microinjection molding technique," *Microsyst Techno. 13*, pp. 517-522.

[23] J. Jiang, J. S. Moore, H. F. Edelhauser, and M. R. Prausnitz, "Intrascleral Drug Delivery to the Eye Using Hollow Microneedles," *Pharm. Res.* Vol. 26, pp. 395-403.

[24] P. Griss and G. Stemme, "Novel side opened out-of-plane microneedles for microfluidic transdermal interfacing," In: *The fifteenth IEEE international conference on micro electro mechanical systems*, pp. 467-470, 2002.

[25] S. Khumpuang, R. Maeda, and S. Sugiyama, "Design and fabrication of coupled microneedle array and insertion guide array for safe penetration through skin," In: *International symposium of micromechatronics and human scienc*, 2003.

[26] E. V. Mukherjee, S. D. Collins, R. R. Isseroff, and L. Smith, "Microneedle array for transdermal biological fluid extraction and in situ analysis," *Sens Actuators A 114*, pp. 267-275, 2004.

[27] N. Wilke, A. Mulcahy, S. R. Ye, and, A. Morrissey, "Process optimization and characterization of silicon microneedles fabricated by wet etch technology," *Microelectron J*, Vol. 36, pp. 650-656, 2005.

[28] T. Shibata, A. Nakanishi, T. Sakai, N. Kato, T. Kawashima, T. Mineta, and E. makino, "Fabrication and mechanical characterization of microneedle array for cell surgery," In: *Actuators and Microsystems Conference*, pp 719-722, 2007.

[29] C. S. Kolli and A. K. Banga, "Characterization of Solid Maltose Microneedles and their Use for Transdermal Delivery," *Pharm. Res.* Vol. 25, pp. 104-113, 2008. 1449-1463, 2001.

[30] M. W. Ashraf, S. Tayyaba, A. Nisar, N. Afzulpurkar, and A. Tuantranont, "Coupled Multifield Analysis of Integrated Microfluidic Device for Transdermal Drug Delivery Applications", In: *INMIC, 13th Multitopic Int. Conf.* 2009.

[31] S. Henry, D. V. McAllister, M. G. Allen, and M. R. Prausnitz, "Micro machined needles for the transdermal drug delivery of drugs," In proc. *IEEE workshop MEMS*, 494-498, 1998.

[32] J. H. Park, S. Davis, Y. K. Yoon, M. G. Allen, M. R. Prausnitz, "Micromachined biodegradable microstructures," In: *16th IEEE Int. Conf. on MicroElectro Mechanical Systems*, Kyoto, Japan 371-374, 2003.

[33] J. H. Park, M. G. Allen, M. R. Prausnitz, "Biodegradable polymer microneedles: Fabrication, mechanics and transdermal drug delivery," J. Contr. Rel., Vol. (104), No. 1, pp. 51-66, 2005.

[34] K. Kim, D. Park, H. Lu, K-H. Kim, JB Lee, "A tapered hollow metallic microneedle array using backside exposure of SU-8," *J. Micromech Microeng.*, Vol. 14, pp. 597-603, 2004.

[35] S. J. Moon, and S. S. Lee, "A novel fabrication method of a microneedle array using inclined deep x-ray exposure," *J. Micromech. Microeng.*, Vol. 15, pp. 903-911, 2005.

[36] J. D. Zahn, N. H. Talbot, D. Liepmann, A. P. Pisano, A.P, "Micro fabricated polysilicon microneedles for minimally invasive biomedical devices," *Biomed. Microdevices 2*: 295-303, 2000.

[37] J. Gere , and S. Timoshenko, Mechanics of materials. Fourth ed. 1997.

[38] W. S. Janna , Design of fluid thermal system, Boston, MA : PWS Pub., 2nd ed. (1998).

[39] N. Wilke , C. Hibert, J. O'Brien, and A. Morrissey, "Silicon microneedle electrode array with temperature monitoring for electropo-ration," *Sensors and Actuators A*. 123-124: 319-325, 2005.

[40] P. Zhang, C. Dalton, G. A. Jullien, "Design and fabrication of MEMS-based microneedles arrays for medical Applications," *Microsyst Technol 15*, pp. 1073-1082, 2009.

[41] Z. Ding, FJ. Verbaan, M. Bivas-Benita, L. Bungener, A. Huckriede, DJ. Berg, G. Kersten and

JA. Bouwstra, "Microneedles arrays for the transcutaneous immunization of diphtheria and influenza in BALB/c mice," *J Control Release*, 136(1), pp. 71-8, 2009.

[42] M. I. Haq, E. Smith, D. N. John, M. Kalavala, C. Edwards, A. Anstey, A. Morrissey, and J. C. Birchall, "Clinical administration of microneedles: skin puncture, pain and sensation," *Biomed Microdevices11*, pp. 35-47, 2009.

Muhammad Waseem Ashraf received Master of Science in Physic from Government College University Lahore, Pakistan and Master of Philosophy in Microelectronics Engineering and Semiconductor Physics from University of the Punjab, Lahore, Pakistan. Currently he is doing Doctor of Engineering in microelectronics at Asian Institute of Technology (AIT), Bangkok, Thailand. His research interests are MEMS, NEMS and Nanotechnology for medical applications. He has won two best paper awards during his PhD.

Shahzadi Tayyaba is currently doing Doctor of Engineering in Microelectronic and Embededd System at Asian Institute of Technology (AIT), Bangkok, Thailand. Previously she did her Bachelor of Engineering and Master of Engineering in Computer Science from UET Lahore Pakistan. Her research interests are artificial intelligence, finite element modeling of materials, micro/nano electromechanical systems for biomedical applications.

Nitin Afzulpurkar is currently an associate professor, Director undergraduate program AIT, and Dean at School of Engineering and Technology, Asian Institute of Technology (AIT), Bangkok, Thailand. He obtained PhD from University of Canterbury, New Zealand in mechanical engineering with specialization in Robotics. He has previously worked in India, NewZealand, Japan and HongKong. He has authored over hundred research papers in the field of Robotics, Mechatronics and MEMS. His current research interests are computer vision, image processing, MEMS, NEMS and mechatronic systems. He is a member of IEEE.

Asim Nisar is currently research scholar in the department of Industrial Systems Engineering (ISE) at the School of Engineering and Technology, Asian Institute of Technology (AIT), Bangkok, Thailand. He completed his PhD in design and manufacturing engineering from Asian Institute of Technology, AIT in Dec 2008. His PhD research dealt with design, analysis and fabrication of MEMS based microfluidic devices for biomedical applications. Previously he has done his master of science in advanced manufacturing technology from University of Manchester, U.K. in 2002. His research interests are micro/nano electromechanical systems and microfluidics.

Erik Lucas Julien Bohez is currently an associate professor in Industrial System Engineering (ISE), Asian Institute of Technology (AIT), Bangkok, Thailand. He done Burgerlijk WerktuigKundig Electro-Technisch Ingenieur, State University of Ghent, Belgium, 1979, Kandidaat Burgerlijk Ingenieur, State University of Ghent, Belgium, 1977 and Technisch Ingenieur, Electro-Mechanica, Higher Technical Institute Saint Antonius Ghent, Belgium, 1976. His research interests are CNC/CAD/CAM , Eco-design, Mold & Die Design and 5-Axis Machining.

Tanom Lomas received the B.Eng. and M.Eng degrees in instrumentation engineering from King Mongkut's Institute of Technology Ladkrabang (KMITL), Thailand. He is a researcher with the Nanoelectronics and MEMS Laboratory, National Electronic and Computer Technology Center (NECTEC), Pathumthani, Thailand. He is also currently doing Ph.D in Faculty of Engineering King Mongkut's Institute of Technology Ladkrabang. His research interests include MEMS, powder blasting, lab on a chip, micromolding and electrooptics.

Adisorn Tuantranont received the B.S. degree in Electrical Engineering from King Mongkut's Institute of Technology, Ladkrabang, Thailand, in 1995, and the M.S. and Ph.D. degrees in Electrical Engineering (Optical MEMS) from the University of Colorado at Boulder in 2001. Since 2001, he has been the Director of the Nanoelectronics and MEMS Laboratory, National Electronic and Computer Technology Center (NECTEC), Pathumthani, Thailand. His research interests are in the area of micro-electro-mechanical systems (MEMS), optical engineering, microfabrication, electro-optics, optoelectronics packaging, nanoelectronics, and lab-on-a-chip technology. He has authored more than 200 international papers and journals and holds five patents. Dr. Tuantranont received the Young Technologist Award in 2004 from the Foundation for the Promotion of Science and Technology under the patronage of H. M. the King.